Chapter 3

Quantifying the Evapotranspiration Component of the Water Balance of Atlantis Sand Plain Fynbos (South Africa)

Nebo Jovanovic, Richard Bugan and Sumaya Israel

Additional information is available at the end of the chapter

http://dx.doi.org/10.5772/53405

1. Introduction

The Cape Floral Kingdom, which experiences the Mediterranean climate of the Western Cape (South Africa), is home to about 9,000 species of the fynbos and succulent karoo biomes, 68% of which are endemic [1]. Vegetation types or veld types of the Cape Floral Kingdom are commonly classified as Mountain Fynbos, Coastal Fynbos, Strandveld and Coastal Rhenosterbosveld. The fynbos biome includes three large taxonomic groups: i) proteoids (tall, deep-rooted shrubs), ii) ericoids (fine leaves, shallow-rooted shrubs), and iii) restioids (graminoids) [2]. Future climate predictions indicate that the Western Cape region will become warmer, drier and subject to more extreme droughts [3,4], with potential risks of species extinctions and range shifts [5]. It is therefore imperative to consider the adaptation mechanisms of these species to drought and their contribution to the water balance as part of a sensitive ecosystem.

The physiological and morphological adaptation of fynbos to drought has been studied in the past. Differences in plant-water relations of two species of Protea (*Protea susannae* and *Protea compacta*) have been previously studied [6]. These two species exhibited different water use adaptation strategies, indicating that habitat specialization plays an important role in their distributions across landscapes. A similar plant-water behavior was observed in different species occurring in riparian zones and hillslopes, as they extract water from deeper soil layers through a well-developed root system [7]. Plant-water relations of several dominant fynbos species were investigated [8], where it was demonstrated that deep-rooted and isohydric species of fynbos tolerate drought better than shallow-rooted and anisohidric species. Rhenosterbos (*Elytropappus Rhinocerotis*) and its impacts on regulating the groundwater table through water uptake via a deep root system were also investigated [9].

The quantification of water resources and the water cycle are of utmost importance in water resources planning and management. This is particularly important in arid regions which experience water stress. In these regions, evapotranspiration (ET) is likely to be the dominant component of the water balance and potential evaporation is much higher than rainfall. It is therefore imperative that ET be accurately quantified. Under such climatic conditions, potential ET rates seldom occur as plants are subject to water shortages and stress due to limited soil water supply. As a physiological adaptation mechanism, plants close stomata resulting in the actual ET rates being below potential rates. This concept of atmospheric demand-soil water supply limited ET was described in detail in [10].

Knowledge of the water use of vegetation could have enormous implications for water resources management. The impact of alien invasive species on streamflow in the Kogelberg area of the Western Cape has been well documented [11]. The results of this study suggested that controlling the spread of alien species in this natural habitat of Mountain Fynbos could reduce water losses by up to 30%, thus increasing the water supply potential of the stream. Groundwater may also be an integral part of the hydrological cycle [12] and shallow groundwater can be a critical resource to natural vegetation [13]. However, the contribution of capillary rise from shallow groundwater to ET is difficult to measure. This study aims to highlight the importance of accurately quantifying ET and also aims to illustrate its effect on other components of the water balance, particularly groundwater recharge. The study was conducted in an area dominated by endemic fynbos vegetation. A lack of data exists, in terms of estimates of ET fluxes from fynbos vegetation, in particular the effects of shallow groundwater on root water uptake. The aim of this study was to quantify all components of the water balance in an area vegetated by Sand Plain Fynbos and characterized by shallow groundwater table. This included weather, vegetation, soil and groundwater. Monitoring from May 2007 to September 2011 served to generate a time series sufficiently long to account for rainfall and weather variability, and for model calibration.

2. Application area

The field trial was established in the Riverlands Nature Reserve, managed by Cape Nature Conservation, located about 10 km South of Malmesbury (Western Cape, South Africa; Figure 1). The reserve is in a predominantly flat area (slope <1%), the soils are deep, well-leached, generally acidic and coarse sandy of marine and aeolian origin (Luvic Cambisol; [14]). The reserve is situated on Cenozoic deposits with Cape granite outcrops occurring in the surroundings. A complete description of the topography, soil physical and chemical properties, and geology was given in [15]. The climate is Mediterranean with the mean annual rainfall being about 450 mm, occurring mainly from May to October. Mean potential annual evaporation is about 2,150 mm and daily evaporation exceeds rainfall for about 70% of the time.

http://dx.doi.org/10.5772/53405

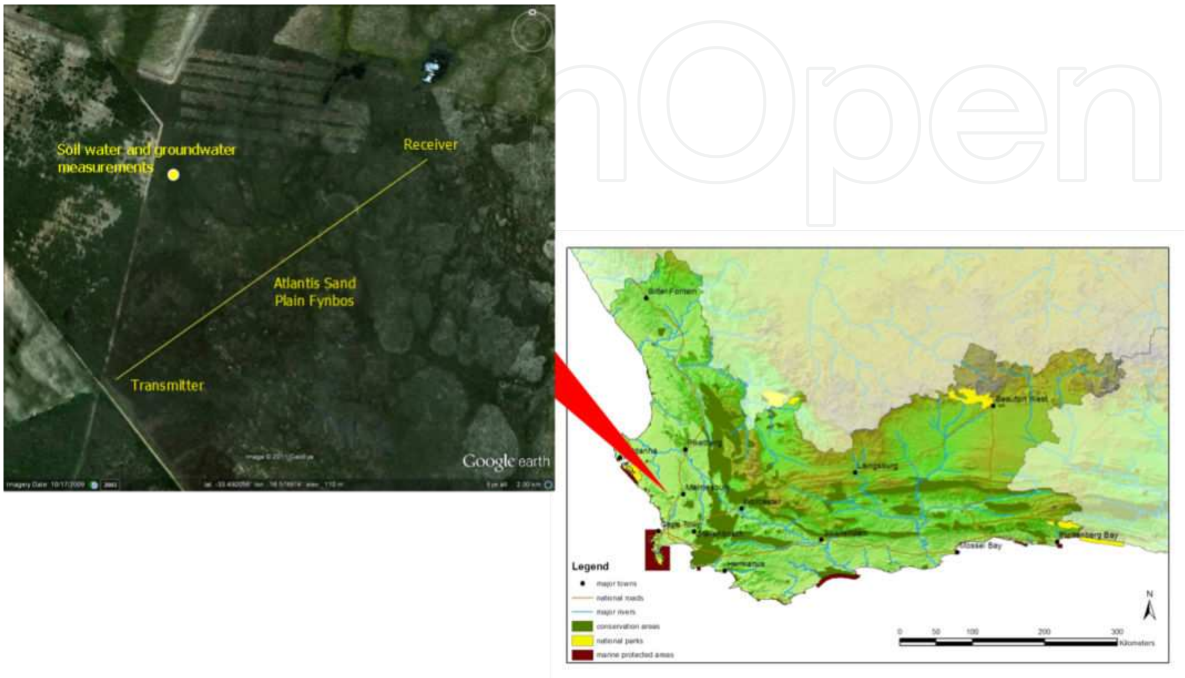

Figure 1. Location of the Riverlands Nature Reserve on the Western Cape map of conservation areas (right). The locations of the scintillometer measurement transect and soil water measurements (yellow circle) are shown in the Google Earth map (left)

The background information for the vegetation description was sourced primarily from [16], and supplemented from [17]. Botanical terminology follows [1] and [16]. The dominant vegetation type of the reserve is Atlantis Sand Plain Fynbos (FFd4, [16]), one of the 11 forms of Sand Plain Fynbos that occurs on the coastal plains of the western and southern coast of the Western Cape. Figure 2 depicts Atlantis Sand Plain Fynbos showing the restio dominated community of the lower-lying areas in the foreground and the taller shrubs of the higher-lying community in the background. The vegetation type is classified as vulnerable with only about 6% conserved, mainly at Pella, Riverlands Nature Reserve (1,111 ha) and Paardeberg. About 40% of the vegetation type has been transformed for agriculture, urban and industrial development, and plantations of eucalypts (for firewood and windbreaks) and pines (windbreaks). Large areas have been invaded by *Acacia saligna* and *A. cyclops* which were used to control drift sands from the mid-1800s up to the 1950s, often in areas that were denuded of vegetation by grazing and excessive burning. The reserve has at least 400 plant species, a number of which are only known from the area.

Figure 2. A view of the Atlantis Sand Plain Fynbos in the Riverlands Nature Reserve

The vegetation is dominated by 1-1.5 m tall emergent shrubs with a dense mid-storey of other shrubs and Restionaceae, a ground layer of recumbent shrubs, herbaceous species, geophytes and grasses with occasional succulents. The Atlantis Sand Fynbos at Riverlands is characterized by a relatively high cover of shrubs of the Proteaceae, Ericaceae and Rutaceae. Shrubs of *Euclea racemosa* and *Diospyros glabra* are also reasonably prominent. The vegetation has two different communities that seem to be controlled by the micro-topography and groundwater depth (Figure 2). Slightly higher-lying areas are dominated by *Protea scolymocephala*, *Leucadendron salignum, Leucadendron cinereum* and *Leucospermum calligerum* with *Erica mammosa*, *Erica* species, *Euclea*, *Diospyros, Phylica cephalantha, Staavia radiata* and shrubs in the Rutaceae. In the lower-lying areas, the dominant species were from the Restionaceae – *Chondropetalum tectorum, Willdenowia incurvata, Staberoha distachyos, Thamnochortus spicigerus* - with *Diastella proteoides, Berzelia abrotanoides, Serruria decipiens* and *S. fasciflora*. The prostate, spreading shrub *Leucospermum hypophyllocarpodendron* (subspecies *canaliculatum*) occurred in both communities, but was more common in the higher-lying areas. The ground layer included a wide variety of geophytic species in the Liliaceae and Iridaceae, seasonal herbs and a few grass species.

3. Method used

The principle of monitoring the entire hydrological system (weather, vegetation, soil and groundwater) was used in this study. Daily weather records for the study period were available from the South African Weather Services (Malmesbury station) and from the Agricultural Research Council (Langgewens holdings of the Western Cape Department of Agriculture). Daily rainfall data were collected with a manual rain gauge at the Riverlands Nature Reserve.

Total evaporation (ET) can be defined as the algebraic sum of all processes of water movement into the atmosphere. Soil evaporation (E) and transpiration (T) occur simultaneously and are determined by the atmospheric evaporative demand (mainly the available energy and the vapour pressure deficit of the air), soil water availability and canopy characteristics (canopy resistances) [18]. Total evaporation is also referred to as ET [19]. In this study, total evaporation represents ET and refers to the sum of evaporation from the soil surface, transpiration by vegetation, and evaporation of water intercepted by vegetation, as estimated with large aperture scintillometers [20]. The energy balance theory and methods for measurement of ET were extensively discussed in [20] and [21].

A Scintec boundary layer large aperture scintillometer system (BLS900, Scintec AG, Germany) was used to estimate fynbos ET in the period 14-27 October 2010. This window period for ET measurements was chosen to be at season change in spring, at a time when both sunny days with high atmospheric evaporative demand and overcast days with low ET occurred.

The BLS900 system measures the path-averaged structure parameter of the refractive index of air (C_N^2) over a horizontal path. The BLS900 system determines C_N^2 and ET over distances of 500 m to 5 km. Estimates of total evaporation are spatially averaged over the area between the transmitter and receiver sensor with a larger proportion of the flux emanating from the middle of the transect. Measurements of C_N^2 together with standard meteorological observations (air temperature, wind speed, air pressure and vertical temperature gradients) collected with an automatic weather station were used to derive the sensible heat flux density (H). The net irradiance was measured using a North – facing net radiometer (CNR1, Kipp & Zonen, Delft, The Netherlands) installed in the middle of the transect over representative vegetation, while the soil heat flux was measured at three different locations within the scintillometer transect using pairs of soil heat flux plates (Campbell Scientific. Ltd, USA) installed at depths of 0.03 and 0.08 m. The latent heat flux (LE) was subsequently calculated as a residual of the simplified surface energy balance equation, from measurements of net irradiance, soil heat flux and H (estimated with the large aperture scintillometer [18]). The assumptions were closure of the surface energy balance and that the energy used for processes like photosynthesis was negligible.

Figure 3 shows the equipment, including the transmitter and receiver of the scintillometer, and the weather station. All data were collected and stored with CR23X data loggers (Campbell Scientific Ltd, USA) for the weather, available energy data and soil heat flux, and in the Signal Processing Unit of the scintillometer for H. The components of the energy balance were measured every half hour. The calculated LE values in W m^{-2} (energy used to evaporate water) were converted into the equivalent water depth units cumulated over the day in mm d^{-1} (ET).

Figure 3. Scintillometer set-up: transmitter (bottom) and receiver (top left) of the scintillometer; and weather station and energy balance system (top right)

The measurements with the BLS900 system were done over a 1,160 m transect indicated in Figure 1. The coordinates at the transmitter were 33.49665 °S, 18.57265 °E and the altitude 114 mamsl. The receiver was located at 33.50103 °S, 18.58454 °E and 111 mamsl. Most of the reserve is relatively young following fires in 2004 and 2005, but the area of ET measurements was situated in a 11-15 years old stand. This compared well with an estimated age of 12-13 years based on counts of shoot growth increments on *Protea scolymocephala* shrubs.

Canopy cover was measured with an AccuPar light sensor in the range of photosynthetically active radiation (Decagon Devices Inc., USA). Readings with the AccuPar were taken in October 2010 at 10 locations along the ET measurement transect (average ratio of 10 readings below the canopy and 10 readings above the canopy). A comparison between readings obtained from manual rain gauges below and clear of vegetation canopy was done in order to estimate canopy interception for rain events in the period between 12/06/2007 and 18/02/2008. Root density was determined in soil samples collected at different depths. A composite soil sample (about 5 kg) was taken from each soil horizon displaying different characteristics down to 0.8 m. The samples were sieved and washed to separate roots from the mineral particles. The roots were then dried in the oven at 40ºC for at least two days. Root density was expressed as mg of dry roots per kg of soil.

Soil water contents were measured at different depths in the profile (0.1, 0.4 and 0.8 m), both adjacent to bushes and in open space areas (Figure 1). Continuous hourly records were collected with Echo-TE sensors and logged with Echo-loggers (Decagon Devices Inc., USA). The location of soil water content measurements was considered to be representative of the scintillometer transect (Figure 1), as vegetation, canopy cover and sandy soil were relatively uniform across the field. The groundwater level was monitored during the study period at shallow monitoring wells equipped with Leveloggers (Leveloggers model 3001; Solinst Ltd., Georgetown, Canada). Surface water, with the exception of occasional ponding in the low-lying areas, did not occur due to the sandy nature of the soil and high infiltration rates.

4. Research course

Well-drained, alluvial, sandy soils are a typical example of a system where vertical water fluxes dominate. Rain water infiltrates in the unsaturated zone, it generates a wetting front and it refills soil layers from the surface towards the bottom of the soil profile. Infiltrating rain water is available for ET. Excess water is drained into deeper soil layers and eventually recharges the unconfined aquifer. The amount of direct groundwater recharge is therefore dependent on initial soil water content, rainfall amounts and distribution, and ET. The main purpose of the experiment at Riverlands was to quantify the various components of the one-dimensional soil water balance (rainfall, soil water storage, evapotranspiration and groundwater recharge/capillary rise). Measurements of rainfall, soil water storage and ET allowed for the quantification of direct groundwater recharge/capillary rise as the residual component of the soil water balance.

A coupled atmospheric-unsaturated zone model was developed to determine the soil water balance of Atlantis Sand Plain Fynbos. The first step in the coupling of models was to apply an atmospheric model to calculate potential evapotranspiration (PET) of Atlantis Sand Plain Fynbos. For this purpose, grass reference evapotranspiration (ETo) was first calculated from weather data with the Penman-Monteith formula [22] and used to determine PET with the following equation:

$$PET = Kc_{max}\ ETo$$

where Kc_{max} is a coefficient dependent on vegetation (i.e. height, morphology) and environmental conditions (i.e. weather variables), and PET represents the evapotranspiration immediately after a rainfall event [22]. Daily PET was then used as input in the unsaturated zone model HYDRUS-2D. Caution should be exercised in the use of this approach for natural vegetation that is usually heterogeneous.

HYDRUS-2D is computer software that can be used to simulate one- and two-dimensional water flow, heat transport and movement of solutes in unsaturated, partially saturated and fully saturated porous media [23]. It uses Richards' equation for variably-saturated water flow and the convection-dispersion equations for heat and solute transport, which is based on Fick’s Law. The water flow equation accounts for water uptake by plant roots through a sink term. The heat transport equation considers transport due to conduction and convection with flowing water, whilst the solute transport equation considers convective-dispersive transport in the liquid phase, as well as diffusion in gaseous phase. The solute flux equations account for non-linear, non-equilibrium reactions between the solid and liquid phases, linear equilibrium reactions between the liquid and gaseous phases, zero-order production and two first-order degradation reactions, the one independent of other solutes, the other providing sequential first-order decay reactions. A dual-porosity system can be set up for partitioning of the liquid phase into mobile and immobile regions and for physical non-equilibrium solute transport. A database of soil hydraulic properties is included in the model. The HYDRUS-2D model does not account for the effect of air phase on water flow. Numerical instabilities may develop for convection-dominated transport problems when no stabilizing options are used, and the programme may crash when extremely non-linear flow and transport conditions occur.

The HYDRUS-2D model allows the user to set up the geometry of the system. The water flow region can be of more or less irregular shape and having non-uniform soil with a prescribed degree of anisotropy. Water flow and solute transport can occur in the vertical plane, horizontal plane or radially on both sides of a vertical axis of symmetry. The boundaries of the system can be set at constant or variable heads or fluxes, driven by atmospheric conditions, free drainage, deep drainage (governed by a prescribed water table depth) and seepage. The HYDRUS-2D version includes a CAD programme for drawing up general geometries and the MESHGEN-2D mesh generator that automatically generates a finite element unstructured mesh fitting the designed geometry.

The HYDRUS-2D model was used to calculate the soil water balance, in particular soil water fluxes towards the groundwater table (i.e. groundwater recharge) and from the shallow groundwater table upwards (i.e. capillary rise). Input data used in the simulations are summarized in Table 1. The main processes simulated were water flow and root water uptake. A vertical plane in rectangular geometry was simulated with a homogeneous profile. The initial condition in water pressure head was established by setting pressure head = 0 at the bottom nodes with equilibrium from the bottom nodes upwards. The hydraulic properties model was van Genuchten-Mualem with no hysteresis. The hydraulic parameters (water flow parameters) were obtained from textural analyses, soil water retention properties and an average bulk density (1.53 g cm^{-3}) [15].

The vertical rectangular dimension of the simulated geometry was 1.5 m, which corresponded approximately to the depth of water table at the beginning of the simulation. The boundary conditions were:

i. Atmospheric top boundary flux (rainfall, potential evapotranspiration).

ii. Constant head = 0 at the bottom nodes to simulate a shallow groundwater table.

iii. No flux at all other boundaries.

Parameters and variables	**Inputs**
Main processes	Water flow, root water uptake
Length units	cm
Type of flow	Vertical plane
Geometry	Rectangular
Number of materials and layers in the soil profile	1
Time units	Days
Initial time	0 (1 May 2007)
Final time	1602 (19 September 2011)
Initial time step	0.05 (default)
Minimum time step	1e-006 (default)
Maximum time step	0.5 (default)
Number of time-variable boundary records	1602
Maximum number of iterations	20 (default)
Water content tolerance	0.0005 (default)
Pressure head tolerance	0.05 (default)
Lower optimal iteration range	3 (default)
Upper optimal iteration range	7 (default)
Lower time step multiplication factor	1.3 (default)

Parameters and variables	Inputs
Upper time step multiplication factor	0.3 (default)
Lower limit of the tension interval	1e-006 (default)
Upper limit of the tension interval	10000 (default)
Initial condition	In the pressure head
Hydraulic model	Van Genuchten-Mualem
Hysteresis	No
Residual water content (Qr)	0.02
Saturation water content (Qs)	0.35
α of the soil water retention function	0.036
n of the soil water retention function	1.56
Saturated hydraulic conductivity (cm d^{-1})	47.85
l of the soil water retention function	0.5
Water uptake reduction model	Feddes
Potential evaporation and transpiration	Daily values calculated from weather data and vegetation characteristics [22]
Horizontal rectangular dimension (cm)	1
Vertical rectangular dimension (cm)	150
Slope of the base	0
Number of vertical columns	2
Number of horizontal columns	150
Mesh	Generated with MeshGen
Root distribution	Uniform down to 1.5 m (bottom of geometry)
Atmospheric boundary condition	Top nodes
Constant boundary condition	Pressure head = 0 at bottom nodes
Initial pressure head	Pressure head = 0 at bottom nodes with equilibrium from the bottom nodes
Depth of observation nodes (cm)	5 and 40 cm

Table 1. Summary of inputs used in the simulation with HYDRUS-2D

The HYDRUS-2D model calculates actual evapotranspiration from PET and applies the method of Feddes to predict reduced transpiration due to water stress. The Feddes' water uptake reduction model incorporated in HYDRUS-2D was used with no solute stress. Actual evaporation from the soil surface was calculated from soil water fluxes at the atmospheric boundary. Observation nodes were set at 0.05 and 0.4 m soil depth to write records of simulated soil water contents. These were also depths of installation of soil water sensors.

5. Results

The canopy cover measured with an AccuPAR in the range of photosynthetically active radiation was between 29.0 and 48.9% (average of 39.2%). The LAI calculated with the AccuPAR varied between 1.12 and 1.54 (average of 1.30). The average rainfall intercepted by the canopy was 0.06%. Intercepted water may have been lost through evaporation or may have reached the soil through leaves and stem flow paths. There were rain events when more water collected in rain gauges below the canopy than in those clear of vegetation. Additionally, the readings obtained under the fynbos canopy were not consistent, indicating that the nature of rainfall and wind conditions may determine the amount of rainfall intercepted by this bushy type of vegetation. The results of the root density measurements are shown in Figure 4. High readings of root density were recorded at about 0.8 m soil depth. This may be indicative of the phreatophytic behaviour of fynbos, with enhanced root development close to the water table. These results, however, need to be confirmed through the analysis of additional samples, given the high spatial variability of plant rooting systems. Given the results and uncertainties of the root density measurements, root distribution was set uniform down to the water table in HYDRUS-2D (Table 1).

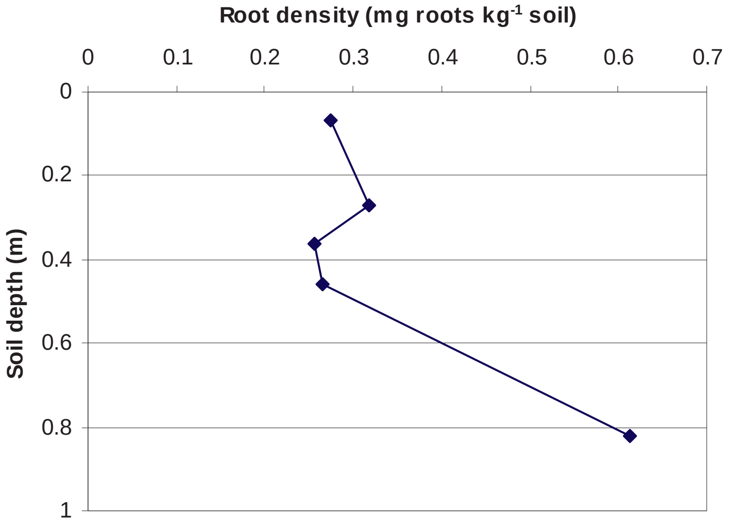

Figure 4. Root density distribution of fynbos

Total evaporation values measured with the scintillometer are shown in Figure 5 for the period 14-27 October 2012. These ET values represent the actual evapotranspiration from an area dominantly vegetated by Atlantis Sand Plain Fynbos. It should however be noted that different vegetation and bare patches also occur at the site. The ET values ranged between 0.8 mm d^{-1} on 21 October 2010 (rainy day) and 5.3 mm d^{-1} on 26 October 2010 (sunny day). High ET values were measured as a considerable amount of water is stored in the soil for ET at the end of the rainy season (14-27 October 2010), a shallow water table occurs (~1.5 m depth on average) and well-established fynbos species have root systems deeper than 0.8 m. Additionally, water stress conditions are interpreted to occur seldom as a result of the shallow groundwater table. The ET values measured in this study could therefore approximate PET of this vegetation. For comparative purposes, ETo calculated with the Penman-Monteith equation [22] was also displayed in Figure 5. The ETo ranged between 2.6 mm d^{-1} (21 October 2010) and 6.8 mm d^{-1} (27 October 2010). The average ratio of ET/ETo for the measurement period was 0.69 with a standard deviation of 0.18.

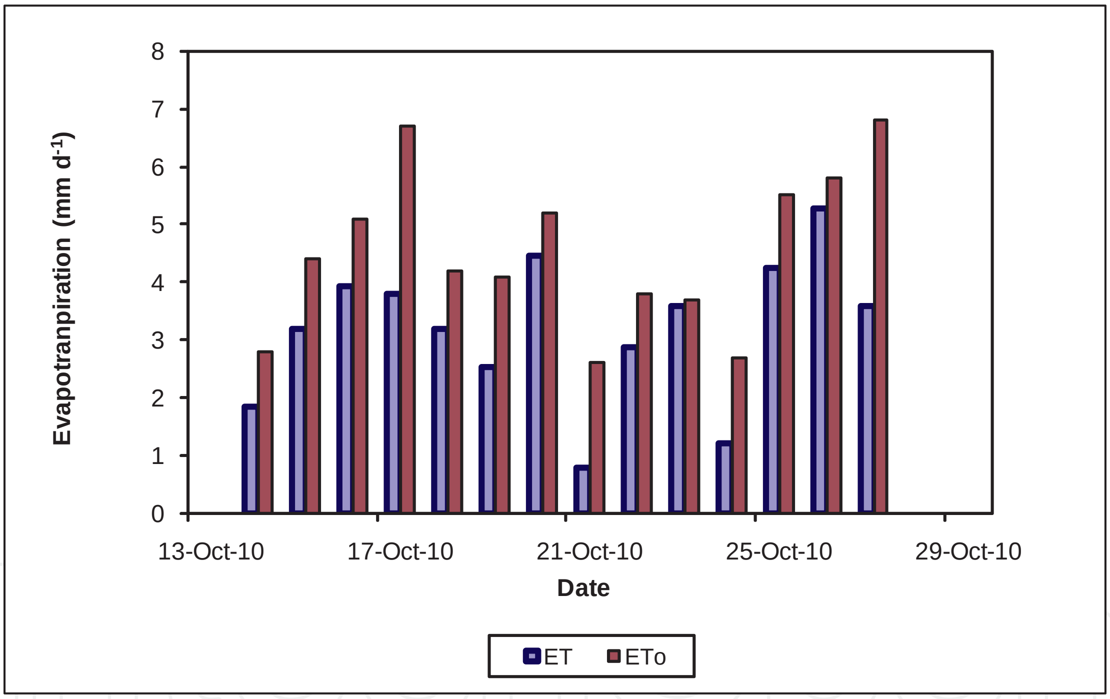

Figure 5. Evapotranspiration (ET) measured with the scintillometer and reference evapotranspiration (ETo) calculated with the Penman-Monteith equation on 14-27 October 2010 at Riverlands

The HYDRUS-2D model was used to simulate direct groundwater recharge and capillary rise as the residual components of the water balance at the study site. Figure 6 shows the daily rainfall data recorded at Riverlands with a manual rain gauge and the cumulative rainfall flux produced by HYDRUS-2D at the atmospheric boundary (input). Total rainfall for the period of simulation from 1 May 2007 to 19 September 2011 was 2,778 mm. The flux units on the Y-axis of the HYDRUS-2D graph represent cm of rainfall. The flux is negative because the water is entering the system.

Figure 7 represents measured and simulated volumetric soil water contents at 0.05 and 0.40 m soil depth. Missing measurements in the first half of 2010 (Figure 7, top graph) were due to logger malfunction. It can be visually noted that the trends and ranges of values obtained with HYDRUS-2D replicated observed measurements very well. As an indication of model performance, this comparison gave confidence in the soil water balance estimation with the model.

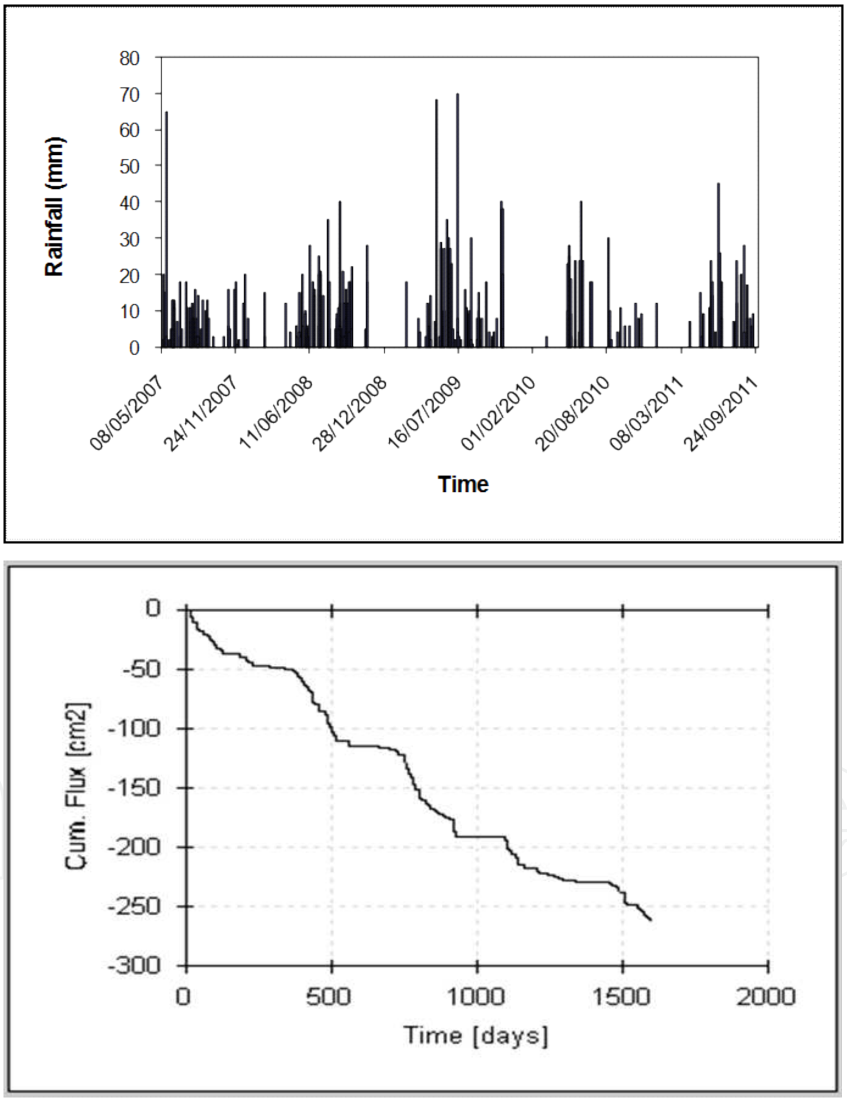

Figure 6. Daily rainfall data recorded at Riverlands with a manual rain gauge (top graph) and cumulative rainfall flux produced by HYDRUS-2D at the atmospheric boundary (bottom graph, screen printout)

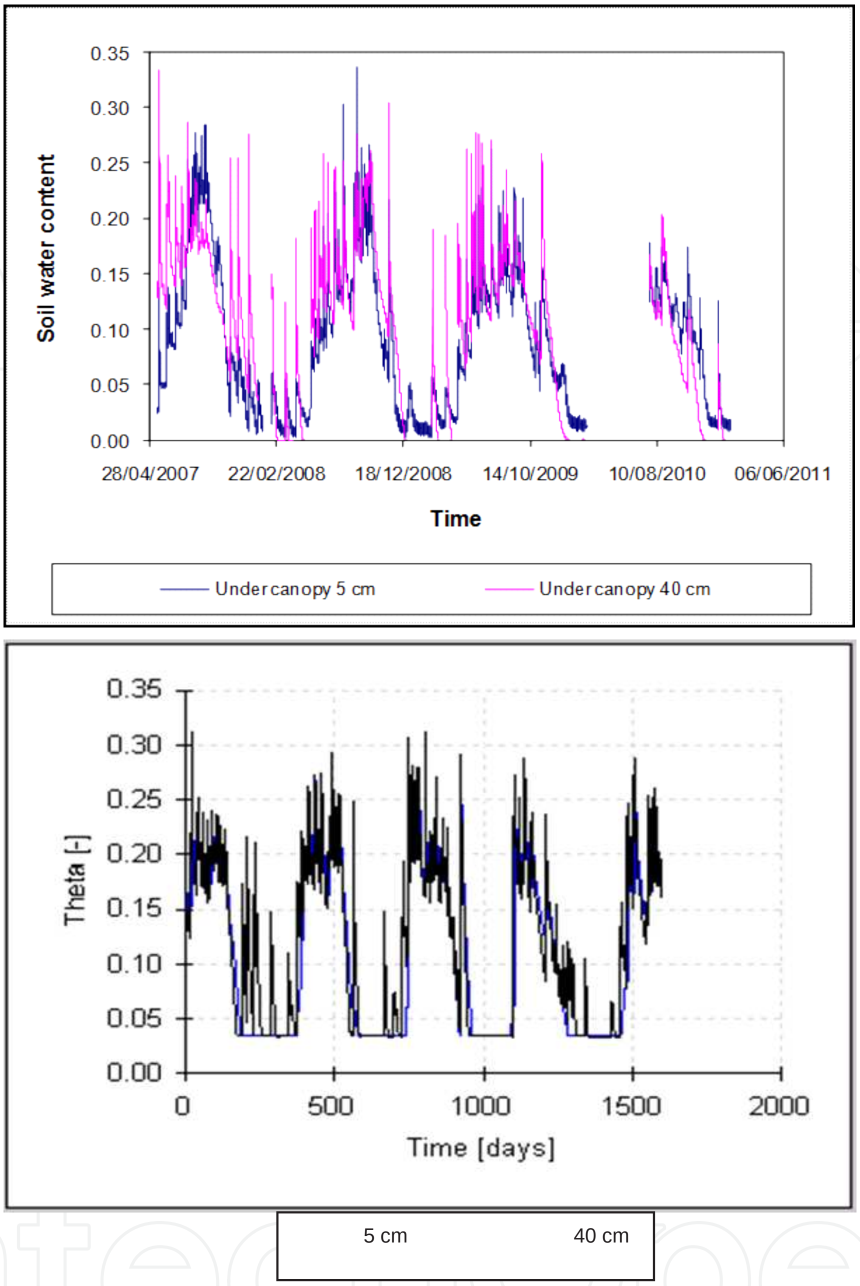

Figure 7. Hourly measurements of volumetric soil water content with Echo sensors (Decagon Inc., USA) (top graph) and volumetric soil water contents (Theta) simulated with HYDRUS-2D (bottom graph, screen printout) at 5 and 40 cm soil depth at Riverlands

The HYDRUS-2D model calculates daily actual ET from PET values by applying the method of Feddes to predict reduced ET due to water stress. The model set-up allowed for root water uptake from the shallow water table by setting a constant pressure of 0 (groundwater table) at the bottom of the soil profile (1.5 m depth). Figure 8 represents HYDRUS-2D output graphs of cumulative potential root water uptake (input) and actual root water uptake calculated with Feddes' model. The fluxes are positive because water is leaving the system. The units on the

Y-axes correspond to cm of root water uptake. Cumulative potential root water uptake for the simulation period was 6,118 mm and actual root water uptake was 4,183 mm (68%). In the two-weeks of scintillometer measurements done in October 2010, the ratio of actual to grass reference evapotranspiration was found to be 69%.

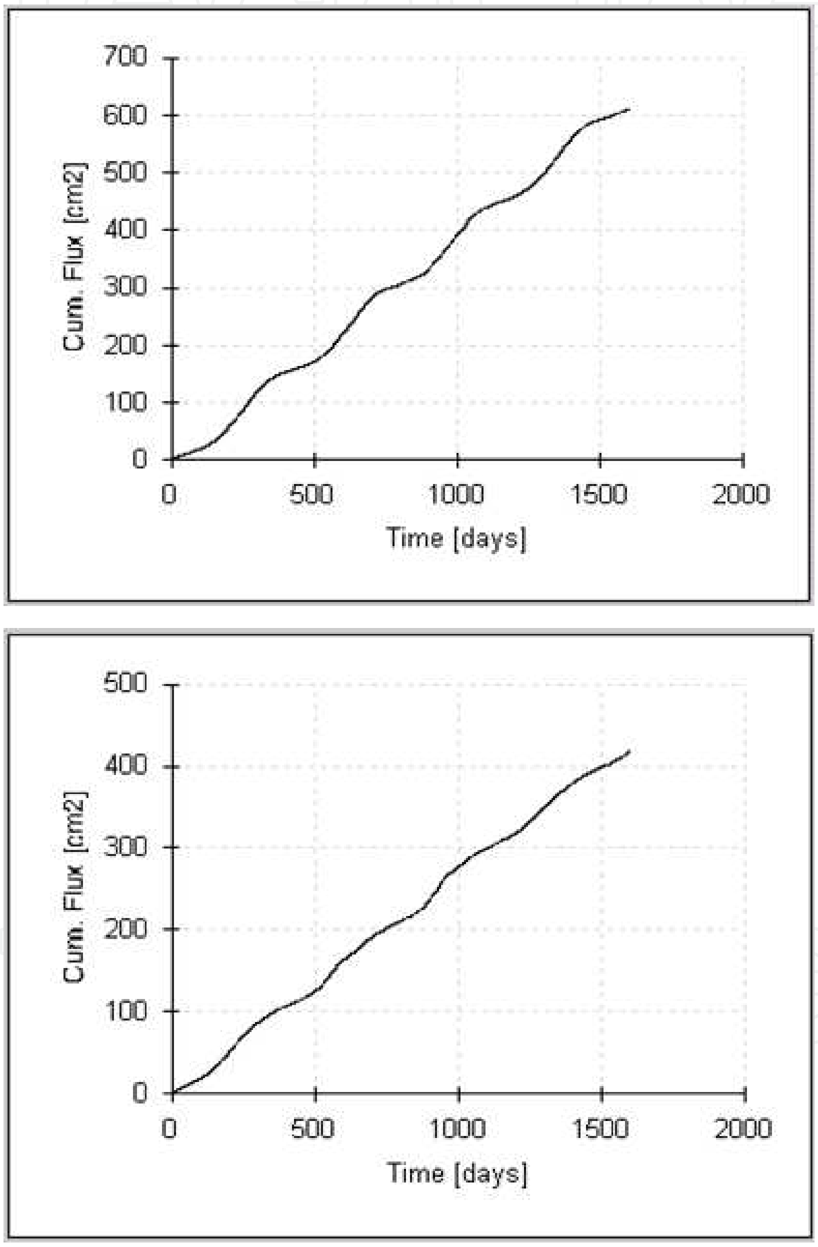

Figure 8. HYDRUS-2D simulations of cumulative potential root water uptake (top graph, input data screen printout) and actual root water uptake calculated with the Feddes' model (bottom graph, screen printout) for fynbos at Riverlands

Figure 9 represents the cumulative fluxes at the bottom boundary (groundwater table). Positive fluxes represent water leaving the system (groundwater recharge) and negative fluxes represent water entering the system (capillary rise from shallow groundwater). The units of the Y-axis correspond to cm. It can be noted that the cumulative flux increased on five occasions (five rainy winter seasons) and it decreased four times (four summers). The increases in flux corresponded to groundwater recharge that occurred during five rainy seasons. Net recharge was largely negative (1,566 mm) because capillary rise from shallow groundwater was much larger than downward water fluxes. Lateral groundwater sources and sinks were not considered in the one-dimensional simulation.

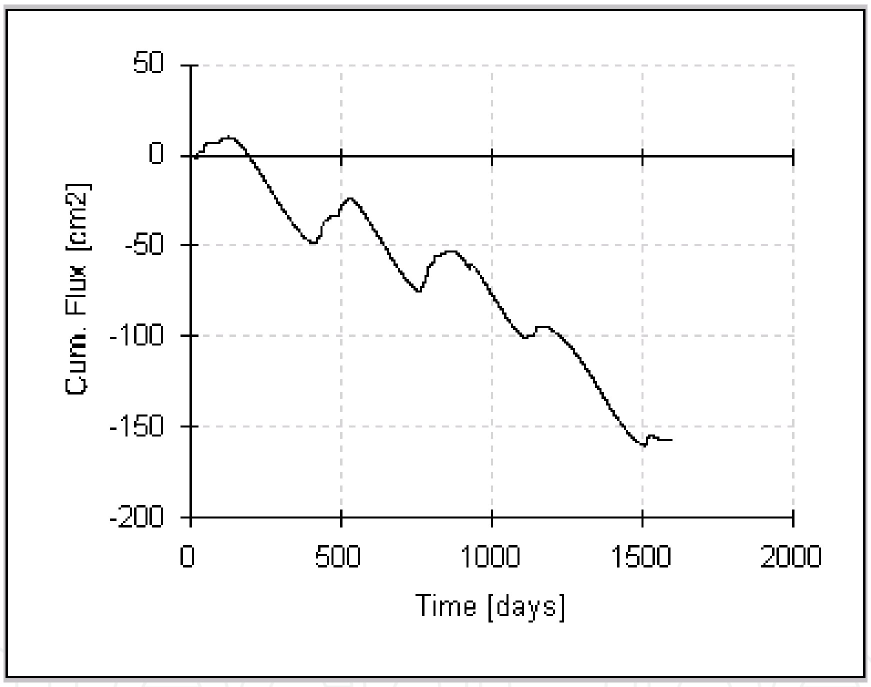

Figure 9. Cumulative bottom boundary flux simulated with HYDRUS-2D (screen printout)

Table 2 presents annual rainfall, groundwater recharge (increases in cumulative flux in Figure 9) and the groundwater recharge as a percentage of rainfall ($R^2 = 0.76$ between annual recharge and rainfall). Comparatively, groundwater recharge in the same catchment was estimated to be 81 mm a^{-1} [24], and 25% of annual rainfall using a mass balance approach at Atlantis (20 km South of Riverlands) [25]. Other estimates of groundwater recharge for the same catchment included 15.4% of mean annual rainfall using a Cl mass balance approach [26], 5% using a GIS-based groundwater recharge algorithm [26] and 13% in the vicinity of Riverlands [27].

Year	Rainfall (mm)	Groundwater recharge (mm)	Groundwater recharge (% of rainfall)
2007	509	98	19
2008	718	253	35
2009	804	227	28
2010	390	65	17
2011	357	55	15
Total	2778	698	25

Table 2. Annual rainfall and groundwater recharge at Riverlands

6. Conclusions and further research

The monitoring of weather, soil water content, vegetation and groundwater was very beneficial in terms of model calibration, to gain understanding of natural systems and ultimately in quantifying water balance processes accurately. This highlights the importance of long term monitored hydrological and hydrogeological data. Scintillometer measurements carried out in October 2010 represented the first direct estimates of ET from Atlantis Sand Plain Fynbos. These measurements were invaluable in gaining understanding of the water use and water balance dynamics of the study area.

The HYDRUS-2D model made good predictions of seasonal variations (trends and ranges) in soil water content in Riverlands. This gave confidence in the soil water balance estimation with the model. Total rainfall for the period of simulation from May 2007 to September 2011 was 2,778 mm. Evapotranspiration rates depended on weather conditions, vegetation (root distribution and canopy cover) and the soil water storage capacity. Cumulative potential root water uptake for the simulation period was 6,118 mm and actual root water uptake was 4,183 mm (68% of the potential and which is approximately equal to the ratio of ET/ETo). The model results also indicated that groundwater contributed considerably to ET, as a result of the fynbos having a well-established root system. The capillary rise from shallow groundwater was simulated to be 1,566 mm more than the downward water fluxes (groundwater recharge). A well-developed fynbos root system at Riverlands allowed the vegetation to tap the shallow groundwater and which resulted in high ET rates. The ratio of simulated actual and potential root water uptake was similar to the ratio of actual (determined using scintillometer measurements) and grass reference evapotranspiration (ET/ETo) during a two-week window period in October 2010.

Uncertainties in the estimates of the water balance components depend on the accuracy of measured input data into the model (e.g. scintillometer measurements, weather data etc.), but especially on temporal variabilities (e.g. rainfall) and spatial variabilities (e.g. rainfall, vegetation, groundwater levels, soil hydraulic properties etc.). For example, the average of 25% of annual rainfall derived for annual direct groundwater recharge (Table 2) should be used with caution as large variations in annual rainfall may result in large variations of recharge (15 to 35% in the five-year time series). It is therefore imperative to account for the seasonality and temporal distribution of rainfall and the other water balance components. Vegetation is spatially variable in terms of canopy cover, structure and speciation. This may have effects on the relation between ETo and PET, root depth and root water uptake and, ultimately, on the water balance. The need to provide an accurate description of the spatial variability of environmental variables (e.g. variability in vegetation) is highlighted. This has implications not only on the estimation of hydrological processes, but also on water management, decision-making and risk associated with the water resource.

A number of recommendations emanated from this research. The study highlighted the need for an accurate conceptualization of the system. The concept of atmospheric demand-soil water supply should be employed in the quantification of actual evapotranspiration. A daily time step is recommended in the calculation of water balance variables to account for daily actual evapotranspiration and rainfall distribution. In some instances, the high temporal resolution of the daily time step can be traded off for speed of calculation (e.g. in numerical models like HYDRUS-2D) and the monthly time step can be adopted to account at least for the seasonality of rainfall and other water balance components. An accurate spatial description of environmental variables is essential (e.g. vegetation, groundwater levels, soil properties etc.). Continuous long-term monitoring of all environmental components (weather, soil water content, vegetation and groundwater) is invaluable for understanding natural systems and calibrating models. Calibration of models should be seen as an on-going process as new data become available. Model sensitivity analyses are essential in order to identify which model parameters are sensitive and which thus need accurate input data. The sensitive parameters in HYDRUS-2D were found to be root distribution, soil properties and potential evapotranspiration. Process models are generally suitable in terms of quantifying the water balance, in particular because computers are able to handle more and more detailed information. However, assumptions, limitations and potential sources of error need to be well-defined (e.g. complexity of systems, interpolation of spatial data, lack and patchiness in input data etc.).

Acknowledgements

The authors wish to acknowledge the Water Research Commission (Pretoria, South Africa) for funding this research, and Cape Nature Conservation for providing the pilot study sites at the Riverlands Nature Reserve and for supplying records of daily rainfall. The South African Weather Services (SAWS) and the Agricultural Research Council are thanked for supplying weather data for Malmesbury and Langgewens, respectively. The authors also thank Dr D. Le Maitre (CSIR, Natural Resources and Environment, South Africa) for the botanical description of fynbos, Dr S. Dzikiti (CSIR, Natural Resources and Environment, South Africa), Dr C. Jarmain and Dr C. Everson (University of KwaZulu-Natal, South Africa) for collecting evapotranspiration data with scintillometry.

Author details

Nebo Jovanovic*, Richard Bugan and Sumaya Israel

*Address all correspondence to: njovanovic@csir.co.za

CSIR, Natural Resources and Environment, Stellenbosch, South Africa

References

[1] Goldblatt P, Manning JC. Plant Diversity of the Cape Region of Southern Africa. Annals of the Missouri Botanical Garden 2002; 89 281–302.

[2] Stock WD, Van der Heyden F, Lewis OAM. Plant Structure and Function. In: Cowling R.M, (ed.) The Ecology of Fynbos: Nutrients, Fire and Diversity. Cape Town, South Africa: Oxford University Press; 1992. p226–240.

[3] Hewitson B, Tadross M, Jack C. Scenarios from the University of Cape Town. In: Schulze R.E. (ed.) Climate Change and Water Resources in Southern Africa: Studies on Scenarios, Impacts, Vulnerabilities and Adaptation. Pretoria, South Africa: Water Research Commission; 2005. p39–56.

[4] IPCC. Pachauri RK, Reisinger A (eds.) Climate Change 2007: Synthesis Report. Geneva, Switzerland: IPCC; 2007.

[5] Hannah L, Midgley G, Hughes G, Bomhard B. The View from the Cape. Extinction Risk, Protected Areas, and Climate Change. BioScience 2005; 55 231–242.

[6] Richards MB, Stock WD, Cowling RM. Water Relations of Seedlings and Adults of Two Fynbos Protea Species in Relation to their Distribution Patterns. Functional Ecology 1995; 9 575-583.

[7] Richardson DM, Kruger FJ. Water Relations and Photosynthetic Characteristics of Selected Trees and Shrubs of Riparian and Hillslope in the South-Western Cape Province, South Africa. South African Journal of Botany 1990; 56(2) 214-255.

[8] West AG, Dawson TE, February EC, Midgley GF, Bond WJ, Aston TL. Diverse Functional Responses to Drought in a Mediterranean-Type Shrubland in South Africa. New Phytologist 2012. doi: 10.1111/j.1469-8137.2012.04170.x

[9] Vermeulen T. Plant Water Relations of *Elytropappus Rhinocerotis* with Specific Reference to Soil Restrictions on Growth. MSc thesis. University of Stellenbosch; 2010.

[10] Jovanovic N, Israel S. Critical Review of Methods for the Estimation of Actual Evapotranspiration in Hydrological Models. In: Irmak A. (ed.) Evapotranspiration – Remote Sensing and Modelling. Rijeka: InTech; 2012. p329-350.

[11] Le Maitre DC, Van Wilgen BW, Chapman RA, McKelly DH. Invasive Plants and Water Resources in the Western Cape Province, South Africa: Modelling the Consequences of a Lack of Management. Journal of Applied Ecology 1996; 33 161-172.

[12] Alley WM, Healy RW, Labaugh JW, Reilly TE. Flow and Storage in Groundwater Systems. Science 2002; 296 1985-1990.

[13] Clarke R, Lawrence A, Foster S. Groundwater: A Threatened Resource. Environment Library No. 15. Nairobi, Kenya: United Nations Environment Programme; 1996.

[14] FAO. World Reference Base for Soil Resources. Rome, Italy: United Nations Food and Agricultural Organization; 1998.

[15] Jovanovic NZ, Hon A, Israel S, Le Maitre D, Rusinga F, Soltau L, Tredoux G, Fey MV, Rozanov A, Van der Merwe N. Nitrate Leaching from Soils Cleared of Alien Vegetation. Report No. 1696/09. Pretoria, South Africa: Water Research Commission; 2009.

[16] Rebelo AG, Boucher C, Helme N, Mucina L, Rutherford MC. Fynbos Biome. In: Mucina L, Rutherford MC. (eds.) The Vegetation of South Africa, Lesotho and Swaziland. Strelitzia 19. Pretoria, South Africa: South African National Biodiversity Institute; 2006. p53-219.

[17] Yelenik SG, Stock WD, Richardson DM. Ecosystem Level Impacts of Invasive *Acacia saligna* in the South African Fynbos. Restoration Ecology 2004; 12(1) 44-51.

[18] Rosenberg NJ, Blad BL, Verma SB. Microclimate: The Biological Environment. 2nd edition. New York, USA: Wiley; 1983. p495.

[19] Kite G, Droogers P. Comparing Estimates of Actual Evapotranspiration from Satellites, Hydrological Models, and Field Data: A Case Study from Western Turkey. Research Report no. 42. Colombo, Sri Lanka: International Water Management Institute; 2000. p32.

[20] Jarmain C, Everson CS, Savage MJ, Mengistu MG, Clulow AD, Walker S, Gush MB. Refining Tools for Evaporation Monitoring in Support of Water Resources Management. Report No. K5/1567/1/08. Pretoria, South Africa: Water Research Commission; 2009.

[21] Savage MJ, Everson CS, Odhiambo GO, Mengistu MJ, Jarmain C. Theory and Practice of Evaporation Measurement, with Special Focus on SLS as an Operational Tool for the Estimation of Spatially-Averaged Evaporation. Report No. 1335/1/04. Pretoria, South Africa: Water Research Commission; 2004.

[22] Allen RG, Pereira LS, Raes D, Smith M. Crop Evapotranspiration: Guidelines for Computing Crop Water Requirements. Irrigation and Drainage Paper 56. Rome, Italy: United Nations Food and Agriculture Organization; 1998. p300.

[23] Simunek J, Sejna M, Van Genuchten MTh. The HYDRUS-2D Software Package for Simulating Two-Dimensional Movement of Water, Heat, and Multiple Solutes in

Variably-Saturated Media, Version 2.0. Riverside, California: U.S. Salinity Laboratory, USDA, ARS; 1999.

[24] Vegter JR. An Explanation of a Set of National Groundwater Maps. Report No. TT74/95. Pretoria, South Africa: Water Research Commission; 1995.

[25] Bredenkamp DB, Vandoolaeghe MAC. Die Ontingbare Grondwaterpotensiaal van die Atlantisgebied. Technical report No. Gh 3227. Pretoria, South Africa: Department of Water Affairs and Forestry, Geohydrology Division; 1982.

[26] DWAF. Groundwater Resource Assessment II: Recharge Literature Review Report 3aA. Project No. 2003-150. Pretoria, South Africa: Department of Water Affairs and Forestry; 2006.

[27] Woodford AC. Preliminary Assessment of Supplying Eskom's Ankerlig Power Station with Water from Local Groundwater Resources. Report No. 374624. Cape Town, South Africa: SRK Consulting; 2007.